

Optimization of a Si-SiO₂ Waveguide Coupler for Photonic Integrated Circuits

Yike Wang

Suzhou University, Suzhou, China

Email: 418570080@qq.com

How to cite this paper: Wang, Y.K. (2018) Optimization of a Si-SiO₂ Waveguide Coupler for Photonic Integrated Circuits. *Circuits and Systems*, 9, 101-106. <https://doi.org/10.4236/cs.2018.97010>

Received: February 26, 2018

Accepted: July 20, 2018

Published: July 23, 2018

Copyright © 2018 by author and Scientific Research Publishing Inc.

This work is licensed under the Creative Commons Attribution International License (CC BY 4.0).

<http://creativecommons.org/licenses/by/4.0/>



Open Access

Abstract

In this paper, we demonstrated a compact Si-SiO₂ waveguide coupler with a footprint of only 2 μm × 3 μm by topology optimization in the communication wavelength. The transmission was increased from 30% to 100%, much higher than other methods. Besides, the optimized structure did not incorporate other dielectric materials, facilitating fabrications and applications.

Keywords

Photonic Integrated Circuits, Topological Optimization, Waveguide Coupler

1. Introduction

Photonic integrated circuits (PICs) integrate multiple photonic functional elements (such as waveguides [1], lasers [2], detectors [3], modulators [4], etc. [5] [6] [7]) to perform a wide variety of advanced optical functions. Progress in other fields such as plasmonics [8], meta-materials [9], etc. has also contributed to the development of PICs. However, there are still some basic issues to be solved with optimization method, instead of using complicated fabrication or intensive parameter search.

In this paper, we first numerically demonstrate that topological optimization could be applied in designing waveguide coupler with near unity efficiency. We designed a new coupler for Si-SiO₂ waveguide transition with high transmission efficiency. 100% transmission is achieved with the design based on topology optimization while introducing minimum modification in the optimization region. This technique could be potentially used in different areas of photonic device design.

2. Model Definition

The topology optimization problem for the Si-SiO₂ waveguide coupler is sche-

matically shown in **Figure 1**. Light at communication wavelength of 1550 nm is launched from the input port made of 430 nm thick Si (with refractive index of 3.5). To get the transmission, the outgoing power is monitored at the output port made of 1.8 μm thick SiO_2 . Other scattered light is absorbed by the perfectly matched layer as indicated between the two dashed lines. To get a high transmission from the Si waveguide to the SiO_2 waveguide, we defined an optimization region of $2 \mu\text{m} \times 3 \mu\text{m}$ in size. The refractive index in this region can vary from 1 to 3.5 according to the following equation.

$$n_{RAMP}(\eta) = \frac{n_{Si} - n_{air}}{1 + \exp[-2p_1(\eta - 0.5)]} + n_{air} \quad (1)$$

where η is the parameter to be optimized directly. p_1 is a control parameter set to be 10 so that over a large range of the value of η , n_{RAMP} is close to either n_{air} or n_{Si} . η is constrained to vary between 0 and 1. n_{RAMP} is chosen this way such that $n_{RAMP}(\eta = 0) = n_{air}$ while $n_{RAMP}(\eta = 1) = n_{Si}$.

Infrared light with 1550 nm is sent from the left input port and transmission is monitored at the output port. Scattered light is absorbed by the perfectly matched layers (the region between the two dashed box).

On the other hand, we still have possibility to get refractive index that is not close n_{air} or n_{Si} in which case, it will be difficult to achieve. We impose another constrain by designating a weight function (w) on every point in the optimization region. The integration over the optimization region is set to be lower bounded by 95% of its area, restricting w to be as close to unit as possible.

$$w = 1 + \frac{1}{1 + \exp[-2p_2(\eta - 0.6)]} - \frac{1}{1 + \exp[-2p_2(\eta - 0.4)]} \quad (2)$$

The Equation (2) shows that w is determined by η which is shown in **Figure 2**, control parameter 1 and control parameter 2 which are defined by **Table 1**. As shown in **Figure 2**, η has different value due to n_{RAMP} and w .

3. Results and Discussions

Figure 3 shows the refractive index (left) and electric field (right) distribution of the original waveguide coupler assuming the optimization region is originally set

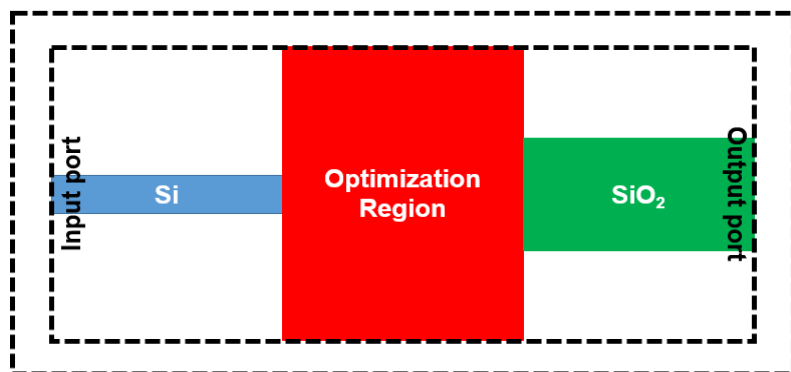


Figure 1. Schematic of the photonic waveguide topology optimization problem.

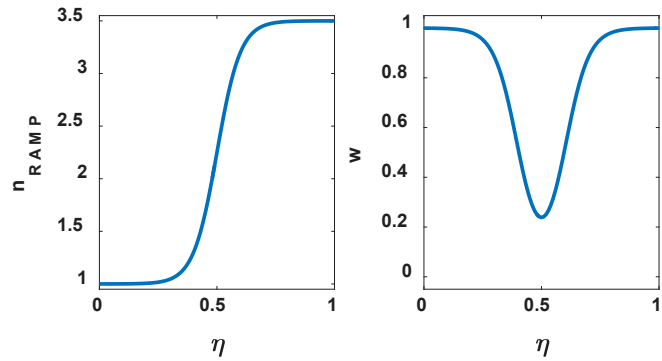


Figure 2. n_{RAMP} and w as a function of η . The two functions are chosen in this way such that the optimized structure tends to choose refractive index of either n_{air} or n_{Si}

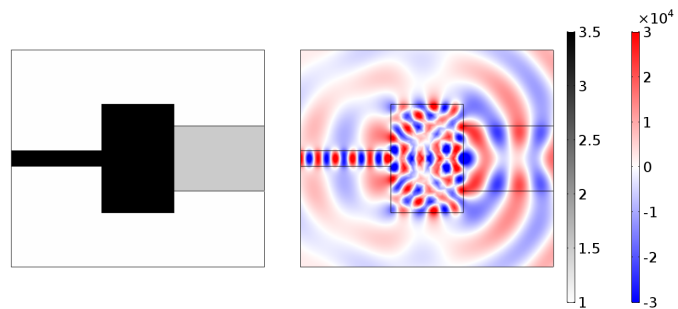


Figure 3. Refractive index (left) and electric field (right) distribution of the original waveguide coupler.

Table 1. Global parameters used in the model to define structures, frequency and temperature.

Lambda	1550 [nm]	Wavelength
W_SiO ₂	1.8 [um]	Width of the SiO ₂ waveguide
W_Si	430 [nm]	Width of the Si waveguide
p ₁	10	Control parameter
p ₂	10	Control parameter
n_SiO ₂	1.5	Refractive index of SiO ₂
n_Si	3.5	Refractive index of Si
n_air	1	Refractive index of air
L_domain	2 [um]	Length of the optimization region
W_domain	3 [nm]	Width of the optimization region
eta_initial	0.8	Initial value of eta
d_PML	0.8 [um]	Thickness of the PML region

to be Si. It is clear that strong scatterings towards unwanted directions and reflection occurs, resulting in only 30% transmission.

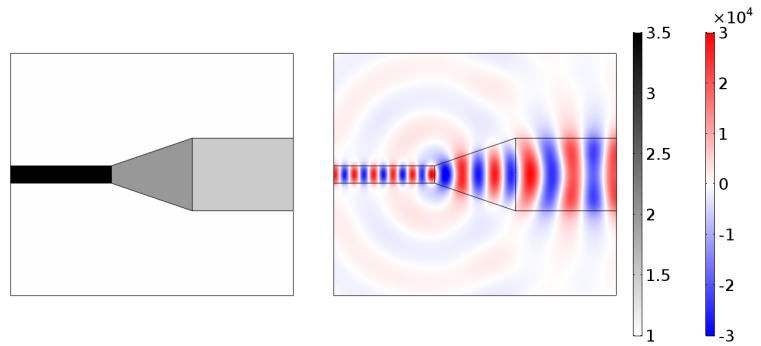


Figure 4. Refractive index (left) and electric field (right) distribution of the waveguide coupler for comparison.

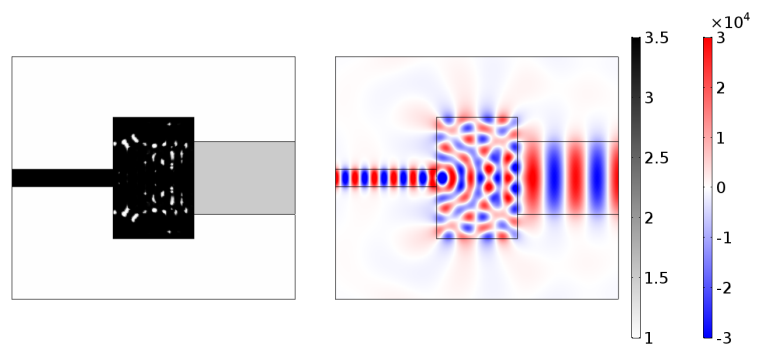


Figure 5. Refractive index (left) and electric field (right) distribution of the topologically optimized waveguide coupler.

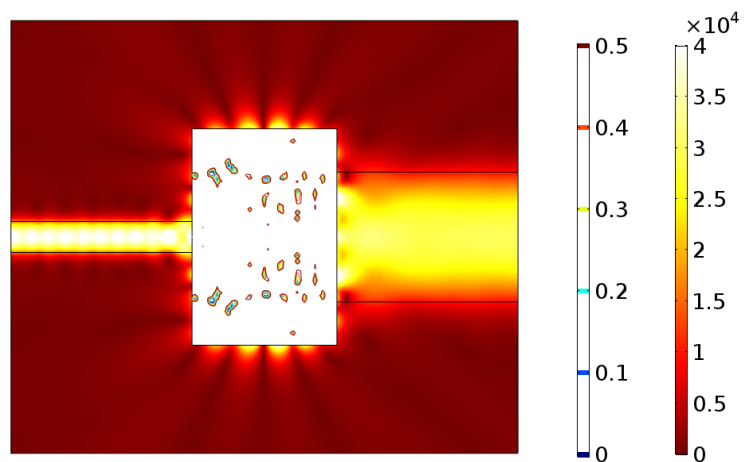


Figure 6. Norm of the electric field distribution outside the optimization region along with contours of $n(x,y) = 0, 0.1, 0.2, 0.3, 0.4$ and 0.5 .

Strong light scattering outside the dielectric region can be observed from the distorted wave front. A transmission of 30% is recorded.

A first step to optimize is to simply introduce a transitional tapered region as shown in the left side of **Figure 4**. The refractive index in the tapered region is chosen to be 2, in between n_{Si} and n_{SiO_2} . Simulation results on right side indi-

cate improved transmission to 72%. Though this is more than twice than the original case, much need to be improved for real applications.

Last, we employ the method described in previous section for topology optimization with results shown in **Figure 5**. Although the refractive index distribution on the left side cannot give us any intuition about the final transmission results, the scattering and interference magically leads to a transmission of 100%, confirming the effectiveness of topology optimization. Moreover in **Figure 6**, we plot the contours of the optimization parameter η ranging from 0 to 0.5. It is clear that the regions between contours of 0.4 and 0.5 is small, indicating most regions with $\eta < 0.5$ has an_{RAMP} close to n_{air} and w close to unit, fulfilling our initial design goal.

Relatively uniform waveguide mode propagation in the input and output waveguide and some scattering outside the dielectric region is observed. A transmission of 72% is recorded.

Uniform waveguide mode propagation in the input and output waveguide and little scattering outside the dielectric region is observed. A transmission of 100% is recorded.

4. Conclusion

In conclusion, we have numerically studied a topological optimization problem for a Si-SiO₂ waveguide coupler in photonic integrated circuits. The design features a compact footprint with minimal region removed. This method could potentially be used in optimization problems of other photonic devices.

References

- [1] Nagarajan, R., Joyner, C.H., Schneider, R.P., Bostak, J.S., Butrie, T., Dentai, A.G., Dominic, V.G., Evans, P.W., Kato, M., Kauffman, M. and Lambert, D.J. (2005) Large-Scale Photonic Integrated Circuits. *IEEE Journal of Selected Topics in Quantum Electronics*, **11**, 50-65. <https://doi.org/10.1109/JSTQE.2004.841721>
- [2] Bergman, D.J. and Stockman, M.I. (2003) Surface Plasmon Amplification by Stimulated Emission of Radiation: Quantum Generation of Coherent Surface Plasmons in Nanosystems. *Physical Review Letters*, **90**, 027402. <https://doi.org/10.1103/PhysRevLett.90.027402>
- [3] Assefa, S., Xia, F. and Vlasov, Y.A. (2010) Reinventing Germanium Avalanche Photodetector for Nanophotonic On-Chip Optical Interconnects. *Nature*, **464**, 80-84. <https://doi.org/10.1038/nature08813>
- [4] Chen, L., Xu, Q., Wood, M.G. and Reano, R.M. (2014) Hybrid Silicon and Lithium Niobate Electro-Optical Ring Modulator. *Optica*, **1**, 112-118. <https://doi.org/10.1364/OPTICA.1.000112>
- [5] Hafezi, M., Mittal, S., Fan, J., Migdall, A. and Taylor, J.M. (2013) Imaging Topological Edge States in Silicon Photonics. *Nature Photonics*, **7**, 1001-1005. <https://doi.org/10.1038/nphoton.2013.274>
- [6] Chrostowski, L. and Hochberg, M. (2015) Silicon Photonics Design: From Devices to Systems. Cambridge University Press, Cambridge. <https://doi.org/10.1017/CBO9781316084168>

- [7] Arakawa, Y., Nakamura, T., Urino, Y. and Fujita, T. (2013) Silicon Photonics for Next Generation System Integration Platform. *IEEE Communications Magazine*, **51**, 72-77. <https://doi.org/10.1109/MCOM.2013.6476868>
- [8] Oulton, R.F., Sorger, V.J., Genov, D.A., Pile, D.F.P. and Zhang, X. (2008) A Hybrid Plasmonic Waveguide for Subwavelength Confinement and Long-Range Propagation. *Nature Photonics*, **2**, 496-500. <https://doi.org/10.1038/nphoton.2008.131>
- [9] Smith, D.R., Pendry, J.B. and Wiltshire, M.C. (2004) Metamaterials and Negative Refractive Index. *Science*, **305**, 788-792. <https://doi.org/10.1126/science.1096796>